Catalysis Today 154 (2010) 68–74

Contents lists available at ScienceDirect

Catalysis Today

journal homepage: www.elsevier.com/locate/cattod

High-resolution fast X-ray photoelectron spectroscopy study of ethylene interaction with Ir(1 1 1): From chemisorption to dissociation and graphene formation

Silvano Lizzit[a], Alessandro Baraldi[b,c,*]

[a] Sincrotrone Trieste S.C.p.A., S.S. 14 Km 163.5, I-34149 Trieste, Italy
[b] Physics Department and Center of Excellence for Nanostructured Materials, University of Trieste, Via Valerio 2, I-34127 Trieste, Italy
[c] Istituto Officina dei Materiali IOM-CNR Laboratorio TASC, AREA Science Park, S.S. 14 Km 163.5, 34012 Trieste, Italy

ARTICLE INFO

Article history:
Available online 17 June 2010

Keywords:
High-energy resolution core level spectroscopy
Iridium
Chemical reactivity
Graphene

ABSTRACT

High-energy resolution fast X-ray photoelectron spectroscopy was used to study the thermal evolution of ethylene on Ir(1 1 1). Temperature programmed photoemission spectra of the C 1*s* and Ir $4f_{7/2}$ core levels were measured in 400 ms/spectrum while ramping the temperature from 170 to 1120 K. The C 1*s* spectra display a large variety of components, assigned to different carbon containing species present on the surface at increasing temperature, namely ethylene, ethylidene, ethylidyne, ethynyl, adsorbed carbon and finally graphene. Components due to the C–H stretch vibration excitation are clearly resolved for C_2H_4, $CHCH_3$ and C_2H_3. The C 1*s* spectra of the last two species display also shifted components that belong to non-equivalent carbon atoms. At temperatures higher than 900 K the narrowing of C 1*s* spectra is caused by graphene formation. Also the Ir $4f_{7/2}$ spectra are strongly affected by the presence of the different species. The clean surface component moves initially towards the bulk peak and shifts back and forth along the series, to recover the binding energy position corresponding to the clean surface when the graphene layer is completely formed. A comparison of ethylene interaction with Ir(1 1 1) and Pt(1 1 1) is presented.

Iridium is a 5d transition metal which exhibits distinctive chemical properties largely employed in several fields, particularly in heterogeneous catalysis. Ir is commonly used to improve the selectivity towards N_2 instead of NO_x production during ammonia oxidation [1]. In addition Ir based catalysts are extensively studied because of their unique catalytic activity for hydrogen production from ammonia and hydrazine [2], free from CO and CO_2, to be used as propellant in satellite propulsion [3]. Moreover, highly dispersed Ir nanoparticles were found to be effective photocatalysts for the production of stoichiometric hydrogen and oxygen by water splitting under visible light irradiation [4].

Because of the high efficiency in C–H bond breaking of small alcohols, such as methanol and ethanol [5], the Ir(1 1 1) surface has recently attracted a lot of attention for the growth of a single graphite layer, named graphene, by hydrocarbon dissociation [6–8]. Whereas the presence of carbon atoms which are not easily hydrogenated, is usually a problem in chemical reactions because it results in surface blockage and catalytic reaction poisoning, the formation of graphene represents a challenge for technological applications in nano-electronics because of the remarkable electronic and transport properties of this two-dimensional carbon system [9]. Because of this, many groups are currently studying different aspects of the graphene on Ir(1 1 1) system, which span from the electronic and structural properties to the understanding of the growth process. A new and atypical growth mechanism was found [10], which involves the creation of dome-shaped carbon nanoislands whose interaction with the Ir substrate takes place only at the cluster edges. It was proposed that this new mechanism of cluster formation, which results in nanosized non-interacting carbon regions, could offer the groundwork for a nanoscale design of graphene-based-systems, in particular for electronic devices making use of quantum dots and nanoribbons [11].

Among hydrocarbons, ethylene is commonly used to produce graphene layers on Ir(1 1 1) with high structural quality. Scanning Tunneling Microscopy (STM) measurements [7,8] have shown that high-temperature ($T > 800$ K) ethylene dissociation results in an incommensurate pattern with a 25.3 Å periodicity and a (9.32×9.32) superstructure, described as a moiré structure. At this temperature the dissociation of C_2H_4 is complete and the interplay between carbon–substrate interaction, surface carbon diffusion

---

* Corresponding author at: Physics Department and Center of Excellence for Nanostructured Materials, University of Trieste, Via Valerio 2, I-34127 Trieste, Italy. Tel.: +39 040 3758719.
E-mail address: alessandro.baraldi@elettra.trieste.it (A. Baraldi).

0920-5861/$ – see front matter © 2010 Elsevier B.V. All rights reserved.
doi:10.1016/j.cattod.2010.05.028

and graphene–Ir lattice mismatch are the key ingredients for the epitaxial growth. What is still missing in these studies is the understanding of the processes that bring a chemisorbed C_2H_4 molecule to break into C_xH_y fragments first, and in a second moment into C atoms, the building blocks of graphene.

It is important to highlight that already in the '70s Nieuwenhuys et al. [12] reported that heating of the Ir(1 1 1) surface above 1070 K in the presence of hydrocarbons results in the formation of a well-ordered carbonaceous overlayer with (9 × 9) periodicity, whose structure was attributed to "*an hexagonal layer of carbon similar to the structure of the basal plane of graphite deposited on the (1 1 1) Ir surface*". Hydrogen thermal programmed desorption (TPD) spectra indicated that C–H bond breaking take place between 370 and 820 K. Later, Marinova et al. [13,14] using high-resolution electron energy loss spectroscopy (HREELS) reported the formation of ethylidyne (C_2H_3) at 180 K, with the C–C axes parallel to the surface. With increasing the temperature above 300 K these species are converted into a new species with the C–C axis inclined. Complete decomposition of ethylidyne into C_2H species was accomplished by annealing to 500 K, thus suggesting a larger activity of Ir(1 1 1) than Rh(1 1 1), Pd(1 1 1) and Pt(1 1 1) surfaces.

In this work we use the high-energy resolution fast X-ray photoelectron spectroscopy (XPS) technique to shed light into the nature of the different chemical precursor species involved in the formation of graphene on Ir(1 1 1) from ethylene. The changes in the C 1*s* and Ir $4f_{7/2}$ core electron binding energies are used to probe the different chemical species present on the surface as well as the local geometric environment of the substrate atoms. By exploiting the tunability and the high brilliance of the soft X-ray radiation produced at third generation synchrotron light sources, which yields an increase of the photon flux of almost three orders of magnitude with respect to conventional anode-based sources, with much higher energy resolution (<50 meV), it is possible to follow *in situ* and in *real time* the modification of the surface composition during a chemical reaction [15]. The same experimental approach was already successfully employed by Fuhrmann et al. [16] to study the dissociation of ethylene on Pt(1 1 1). Binding energy changes and vibrational signatures of the C 1*s* spectra were used to make the assignment of the different surface species, in particular ethylidyne which forms on Pt(1 1 1) at 290 K and another intermediate species which was tentatively assigned to ethylydene ($CHCH_3$).

The Ir sample, a 6 mm diameter disc oriented along the (1 1 1) direction within 0.1°, was cleaned by repeated cycles of Ar^+ sputtering (T = 300 K, E = 2.5 keV), annealing at 1470 K, oxygen treatments (T = 570–970 K, $p = 1 \times 10^{-7}$ mbar) and a final annealing in H_2 to remove residual oxygen (T = 370–670 K, $p = 1 \times 10^{-7}$ mbar). This procedure yielded a very well ordered and clean surface, as proved by the sharp and low background (1 × 1) low energy electron diffraction (LEED) pattern and by the absence of traces of contaminants in the C 1*s*, S 2*p* and O 1*s* core level regions (detection limit below 0.5% of a monolayer).

The core level photoemission measurements were performed at the SuperESCA beamline of the synchrotron radiation source Elettra in Trieste. C 1*s* and Ir $4f_{7/2}$ core level spectra were acquired at photon energies of 400 and 130 eV, respectively. A Phoibos hemispherical electron energy analyser from SPECS (mean radius of 150 mm) implemented with an home-made delay-line detection system, was used to collect the spectra. The technology of the delay-line detector allows for acquisition times in the ms range when running the analyser in the so-called snap-shot mode, with thousand energy data points per spectrum. The C 1*s* and Ir $4f_{7/2}$ core level spectra of the present work were acquired in 400 ms.

The high sensitivity to the local environment of the narrow C 1*s* and Ir 4*f* core levels, together with the high-energy resolution available (60 and 40 meV for the C 1*s* and Ir 4*f* spectra, respectively), allowed us to perform Temperature Programmed XPS (TP-XPS) experiments [17]. We measured very high quality C 1*s* and Ir $4f_{7/2}$ spectra with unprecedent speed from 180 to 1120 K with a linear ramp of 1.5 K/s. Such a wide temperature range allowed us to follow the dissociation pathways of ethylene till the formation of a well ordered, almost free-standing graphene layer on Ir(1 1 1).

C_2H_4 was dosed onto Ir(1 1 1) kept at 170 K at a background pressure of 1×10^{-7} Torr for 300 s, corresponding to 30 Langmuir (L), to ensure saturation of the surface.

The C 1*s* and Ir 4*f* binding energies are referred to the Fermi level, measured under the same experimental conditions (photon energy, analyser set-up and surface temperature). The photoemission spectra were fitted by convoluting a Doniach–Šunjić (DS) function [18] with a Gaussian to account for the vibrational-unresolved broadening and the instrumental resolution. A linear background was also subtracted. The DS profile contains a Lorentzian distribution arising from the finite core–hole lifetime, and an asymmetry parameter for electron–hole pair excitations at the Fermi level. The C 1*s* lineshape parameters (Lorentzian and Gaussian width and asymmetry) for the different species present on the surface, as well as the distance between the peaks that belong to the same chemical species, were optimised at some selected temperatures and then fixed during the analyses of the TP-XPS data, while the intensities were allowed to vary. It is important to note that the Gaussian width of the individual components can be different not only because of vibrational effects, but also because of inhomogenous broadening. This effect arises from the different local configurations and it is particularly relevant for the atomic carbon species resulting from molecular dissociation at high temperature, as reported in our previous work [10]. The BE positions were also let free, with the constraint explained above.

Fig. 1(a) shows a two-dimensional plot of the time-lapsed C 1*s* spectra acquired while heating the Ir(1 1 1) surface saturated with ethylene at 170 K. The intensity, represented as a density plot by a colour scale, ranges from low (blue) to high (white). The large intensity variations are a clear fingerprint of the presence of distinct features at different BEs.

Fig. 1(b) shows a sequence of C 1*s* spectra at different temperatures, selected from the complete TP-XPS series to figure out the evolution of the surface layer. In the following the fitting procedure as well as the interpretation of the different components are explained in more detail.

The first C 1*s* spectrum of Fig. 1(b) (spectrum (1)) measured at 190 K displays three main components at BE of 282.56, 283.26 and 283.67 eV. While at a first sight only three components are visible, other two extra peaks at 283.06 and 283.83 eV have to be included in the fit in order to achieve a small residual with low modulation. This is confirmed by the fit of the spectrum measured in scanning mode with higher statistics (not shown) just after ethylene adsorption at 170 K before starting the TP-XPS experiment. One has to bear in mind that sharp, well-resolved core level components emerging in the C 1*s* spectra are not necessarily associated with non-equivalent C species, but are expected also because of vibrational excitations of C–H stretching modes in the final state. Hydrocarbons adsorption on transition metal surfaces often results in multi-component C 1*s* spectra related to this effect [16,19–21].

At higher temperature (spectrum (2)) the low BE components (A, shown in black) disappear and only the three higher binding energy peaks (B, shown in grey) are present, shifted by ~30 meV to higher BE with respect to spectrum (1). The intensity behaviour of the different components as obtained from the analysis clearly indicates that the relative weights of the two peaks in the low BE region and of the three high BE components, are constant such that they behave as a doublet and a triplet, respectively. Let us discuss now what is the meaning of the individual peaks.

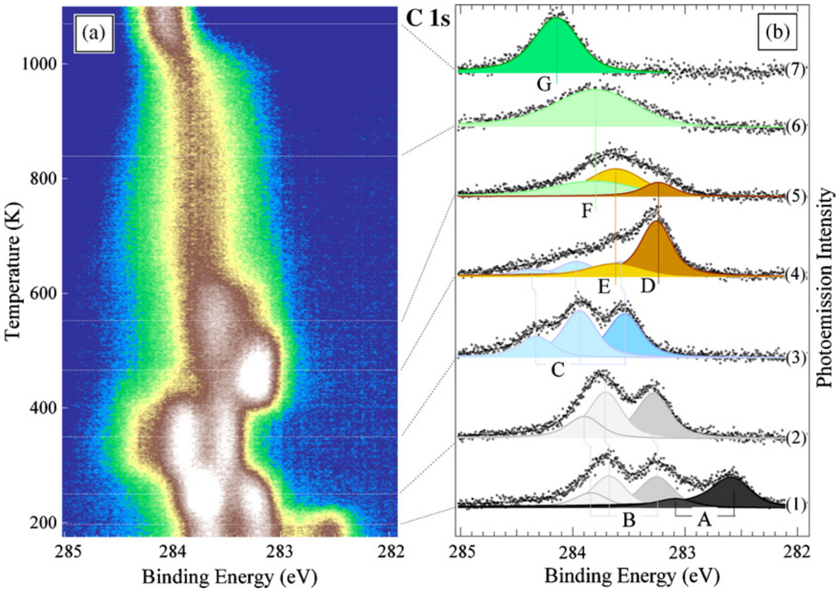

Fig. 1. C 1*s* core level spectra acquired during thermal evolution of the ethylene layer prepared by dosing 30 L of C_2H_4 at 170 K. The photoemission intensities are represented using a coloured density plot scale ranging from low (blue) to high intensities (white). (b) Selected C 1*s* spectra measured at different temperatures. Coloured peaks show results of a deconvolution into different contributions corresponding to inequivalent carbon atoms and vibrational excitations, as discussed in the text. (For interpretation of the references to colour in this figure legend, the reader is referred to the web version of the article.)

Starting with spectrum (2), the intermediate component cannot be attributed to a vibrational excitation relative to the component at low BE because their ratio is ∼1. In fact, the S-factor for hydrocarbon molecules, i.e. the ratio of the area of the first vibrational peak to the adiabatic component which can be calculated using the linear coupling model [22], must be always less than ∼0.5. This implies that the two low BE components of the triplet are associated to non-equivalent carbon atoms of the same molecule, while the higher BE peak is attributed to a vibrational excitation of the central peak. Similar considerations can be applied when examining the doublet A of spectrum (1). However, while the S-factor of doublet A is 0.3 ± 0.1, that of triplet B is 0.5 ± 0.1. These values are related to the number of C–H bonds which, in the case of A turns out to be most probably two while for B is three. The error bars in the determination of the splitting of the A and B components (which is about 0.1 eV) are quite large because of the overlap of the different spectral contributions. Indeed in a range of less than 3 eV five different components are present: even though the energy resolution is set at 60 meV for C 1*s* spectra, the natural core–hole lifetime and the finite vibrational broadening do not permit to determine the evolution of these species with higher accuracy when measuring in snap-shot XPS mode.

From the above considerations it is realistic to explain doublet A as due to ethylene molecules which, at 170 K, chemisorb on Ir(1 1 1) partly intact and partly transform into a different species, B, that we attribute to ethylidene ($CHCH_3$). This assignment is based on previous findings on the conversion of ethylene to ethylidyne on Pt(1 1 1) [16,23,24], where ethylidene was invoked as intermediate species.

However, energy loss experiments on the adsorption of ethylene and acetylene (C_2H_2) on Ir(1 1 1), detected the presence at relatively low temperature of both CH or CCH species on the surface. Therefore these species as well may contribute to the spectral features assigned to ethylidene. It is worth noting that the expected vibrational splitting of the CH_3 group should be of the order of 400 meV and that the spectrum of ethylidene should present the vibrational components of both CH and CH_3 groups, with a weight proportional to the number of H bonds. This last component was not included in the analyses in order not to overfit the data. This, together with the presence of chemical species other than ethylidene may be the reason of the relatively small CH_3 vibrational splitting found for species B.

A slight increase of the temperature to 235 K results in a complete transformation of ethylene into ethylidene.

In the relatively narrow temperature range from 235 to 250 K the spectra are dominated by the ethylidene features. Above 250 K three new components (C of spectrum (3)) grow and reach a maximum at ∼310 K setting at BE of 283.53, 283.93 and 284.32 eV, when ethylidene has completely disappeared. As for the ethylene- and ethylydene-induced C 1*s* components the ratio between the three peaks remains always constant. Components C behave then as a triplet. We propose therefore that these peaks originate from the same molecule, which adopts always the same local geometry when bonded to Ir(1 1 1). Being unlikely the formation of intermediate species with three chemically non-equivalent C atoms, we attribute the higher BE peak to the vibrational excitation related to the central component. By comparison with previous XPS results on the dissociation of ethylene to ethylidyne on Rh(1 1 1) [19], where two distinct C 1*s* species were measured, we assign the two carbon species of the present case to ethylidyne molecules (CCH_3) adsorbed on the Ir(1 1 1) surface in upright configuration. Our interpretation is supported by the value of the S-factor, which results to be, as in the ethylidene case, equal to 0.5 ± 0.1, thus suggesting that a triple C–H bond is present. The S-factor is in good agreement with the value reported in Ref. [16] for the Pt(1 1 1) case. Moreover the separation of 390 meV between the adiabatic and first excited peak is in good agreement with the literature value of 394 meV reported for ethylidyne adsorbed on Rh(1 1 1), a result which indicates the weakening of the C–H bonds in the core-ionized ethylene molecules when adsorbed on Ir with respect to Rh.

The C 1*s* spectrum undergoes further modification upon heating the surface above 400 K where most of the spectral intensity moves towards lower BE. A new sharp component (D of spectrum (4)) grows at 283.25 eV, while a broad feature (E) at 283.56 eV has to be included in the analysis to correctly fit the whole sequence between 400 and 650 K. The intensity gain of the D component is paralleled by a decrease and a shift of 30 meV to higher BE of the triplet C, which disappears at about 550 K. It is interesting to note that these temperatures correspond to the desorption of molecular hydrogen after ethylene exposure at room temperature, as reported by Nieuwenhuys et al. [12]. They found the onset for H_2 desorption to be at ~370 K and a main desorption feature at ~480 K. This is a clear sign of the dehydrogenation process taking place on C_2H_3 molecules. The two temperatures reported in the TPD experiments correspond to the onset and to the maximum of the D component, respectively. In this temperature range, the HREELS data [13] show a vibrational feature at $1260\,cm^{-1}$, interpreted as a ν-CC stretching mode, thus arising from surface species containing at least two carbon atoms. This was tentatively explained as a consequence of ethylidyne dehydrogenation to C_2H. Following this interpretation we assign peak D to ethynyl species.

The second hydrogen desorption feature revealed in TPD experiments [12] has a maximum at ~630 K and extends up to ~730 K. This behaviour nicely compares with that of component E (spectra (4) and (5)) and indicates the dehydrogenation of the corresponding species as a function of temperature. We draw therefore the following scenario: the dehydrogenation process of ethylidyne starts with the formation of C_2H (component D) already at 370 K. Then peak E starts to grow as a result of the conversion of D without dehydrogenation of the corresponding C_2H. We assign therefore the E component to C_2H species most probably sitting in a different adsorption site and/or with a differently oriented C–C axis. It is important to note that at this temperature any attempt to reveal vibrational features in the core level spectra was unsuccessful because of spectral broadening and of the co-adsorption of different species.

The last temperature-induced dehydrogenation step of the C_2H species starts at ~500 K when a broad C 1*s* component emerges at 283.77 eV BE (spectrum (6) of Fig. 1(b)). The increase of this component is paralleled by a drop of the signal associated to C_2H (component E). According to the TPD data of Nieuwenhuys et al. [12] the molecules are completely dehydrogenated at ~800 K, in very good agreement with our photoemission data [10]. Indeed we have recently found that carbon formation and its diffusion above 550 K are the key ingredients for the creation of graphene islands. The large Gaussian contribution of the E and F components, when compared with that of lower temperature surface species, is attributed not only to temperature effects, but also to a wide distribution of atomic carbon configurations, as previously found [10]. The conversion from carbidic carbon, which contributes to the F components, to a low interacting graphene layer proceeds via formation of dome-shaped carbon nanoislands whose interaction with the Ir substrate takes place only at the cluster edge. The existence of these islands with unusual morphology explains the broadening of the C 1*s* (component F), preceding the formation of the graphene layer, characterized by a narrow C 1*s* peak, even when measured at very high temperature (spectrum (6) of Fig. 1(b)). Indeed the atoms at the periphery of the cluster, just bonded to two carbon atoms show a negative core level BE shift with respect to the atoms at the center of the islands, while the carbon atoms directly bonded to the periphery atoms show a positive shift. When the Ir(1 1 1) surface is finally annealed above ~950 K the growth of the component at 284.12 eV (G peak of spectrum (6) in Fig. 1(b)) is associated to the formation of a quasi free-standing graphene layer, which displays a typical moirè pattern, firstly observed in LEED experiments by Nieuwenhuys et al. [12].

The detailed quantitative analysis of the TP-XPS spectra shown in Fig. 1, is displayed in Fig. 2, where the contribution of the components due to inequivalent C atoms and vibrational excitations corresponding to the same chemical species are added together.

It can be noticed that the overall photoemission intensity diminishes at higher temperature. Photoelectron diffraction effects, together with variations of the atomic density, can give rise to modulations of the core level photoemission intensity. This contribution can be very large, in particular for the molecular system of the present investigation where strong forward scattering effects take place along the C–C bond direction. For these reasons our results are in agreement with previous TPD data where only a very small amount of C_2H_4 was detected as desorbing species [12].

The large variations of the chemical composition of the layer observed in the TP-XPS experiment on the C 1*s* core level, give rise to substantial and measurable changes also to the Ir $4f_{7/2}$ spectra. Fig. 3 displays the spectra of a TP-XPS experiment on Ir $4f_{7/2}$ similar to the one performed on the C 1*s*. The measurement of the substrate core levels in transition metal surfaces represents in fact a powerful approach to understand the changes in the adsorbate–substrate interaction [25]. Indeed the core level BE of the first-layer transition metal atoms is different from the bulk, giving rise to the so-called surface core level shifts (SCLS). SCLSs, even if usually relatively small being in the order of some hundreds meV, can be measured with high precision for both clean and adsorbate covered surfaces by combining the high-energy resolution of modern electron energy analysers with the use of soft X-ray monochromator based beamlines.

The SCLS of clean Ir(1 1 1) is mainly due to the reduced coordination of the surface atoms with respect to the bulk, which results in a narrowing of the surface *d*-band around its centroid. In order to keep surface and bulk atoms at the same chemical potential, an electrostatic potential appears at the surface which shifts the *d*-

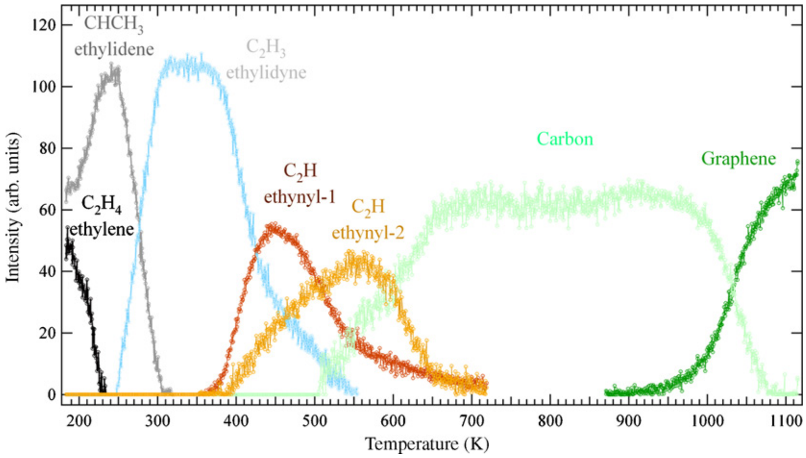

Fig. 2. Quantitative analysis of the thermal evolution of the different surfaces species. The contribution of the components due to inequivalent C atoms and vibrational excitations corresponding to the same chemical species are added together.

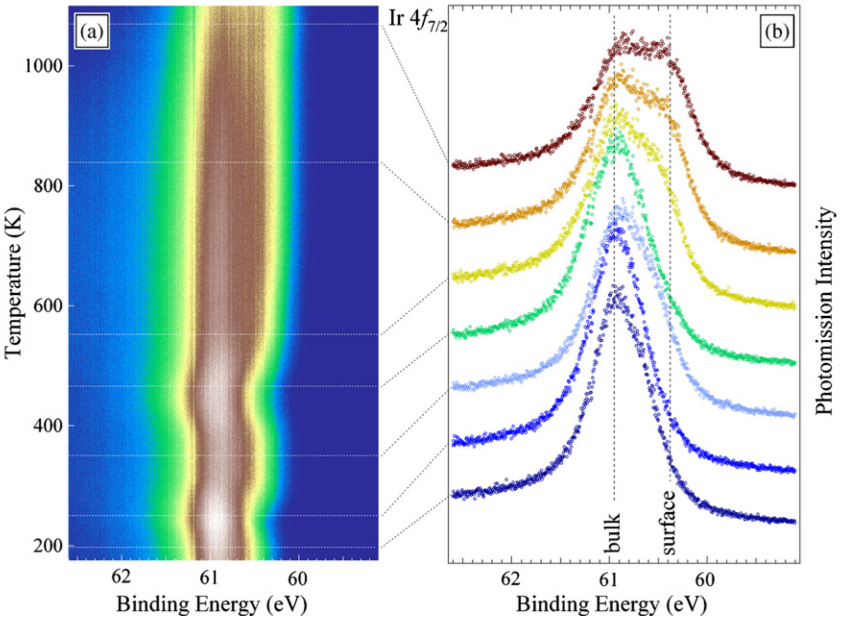

Fig. 3. Ir $4f_{7/2}$ core level spectra acquired during thermal evolution of the ethylene layer prepared by dosing 30 L of C_2H_4 at 170 K. The photoemission intensities are represented using a coloured density plot scale ranging from low (blue) to high intensities (white). (b) Selected Ir $4f_{7/2}$ spectra measured at different temperatures. The binding energies of the surface and bulk components corresponding to the clean Ir(1 1 1) spectrum are also reported with dotted lines. (For interpretation of the references to colour in this figure legend, the reader is referred to the web version of the article.)

band as well as the deep core levels towards lower BE in the case of a more than half-full *d*-band like Ir. The SCLS of Ir(1 1 1) turns out to be −550 meV [26]. Upon ethylene adsorption at 170 K the Ir $4f_{7/2}$ spectrum clearly shows the vanishing of the clean surface component which moves towards the bulk component, apparently resulting is a single peak with a shoulder at low BE. A similar, though quantitatively different shift of the surface component appears in all the spectra acquired up to a temperature of about 500 K, the narrowest peak being in the presence of ethylidene and the broader with ethylidyne. This trend can be explained in terms of changes of the Ir valence 4*d*-band projected onto the surface atoms. It is well known that upon atomic and molecular adsorption, the creation of bonding and anti-bonding states results in an overall broadening of the *d*-band [27–30] and a lowering of the density of states in the Fermi level region. This results in a *d*-band center shift towards higher binding energies, which is reflected also in $4f_{7/2}$ SCLS. What is intriguing is that, in the presence of the different species on the surface, as determined from the C 1*s* spectra, the BE shift of the Ir $4f_{7/2}$ surface component undergoes significant changes. In particular, in presence of ethilydyne the induced shift to the clean surface component is minimum, because a pronounced shoulder is present at low BE, thus indicating on average a low adsorbate–substrate interaction. On the contrary a largest shift is induced by ethylene and, even larger by ethylidene where no shoulder can be distinguished at low BE. A possible explanation of this trend could be found by considering the case of ethylidyne adsorption on Pt(1 1 1) [31], where a $p(2 \times 2)$ layer is formed by C_2H_3 molecules occupying three-fold fcc sites, thus letting 1/4 of Pt surface atoms uncoordinated. This would produce a Pt $4f_{7/2}$ spectrum showing an extra component relatively close to the bulk peak, due to Pt atoms bound to ethylidyne and a small peak shifted to low BE due to the clean surface atoms. However, such a reasoning cannot be easily applied to our Ir $4f_{7/2}$ TP-XPS data because of the complexity of the system at temperatures lower than 700 K due to the presence of different coadsorbed species or, at low temperature, due to the presence of hydrogen which is known to induce substantial changes to the SCLS of transition metals [32–35]. What is evident from Fig. 3 is that above 550 K the clean surface component, associated to unperturbed first-layer Ir atoms, continuously grows with temperature. Even if the phonon-induced broadening results in an increase of the Gaussian width of the bulk and surface peaks, the effect of the heating is the formation of two well-resolved peaks, with a BE difference of about −530 meV, i.e. very close to the SCLS of the clean surface of −550 meV. This is a clear fingerprint of graphene formation, as we have previously determined by comparing photoemission measurements with density functional theory calculations [10]. Indeed, the presence of a complete and well-ordered graphene layer on Ir(1 1 1) does not alter appreciably the electronic structure of Ir first-layer atoms, because of the small interaction that results in a large distance of about 4 Å between graphene and the Ir substrate. This makes the Ir $4f_{7/2}$ spectra of the clean and graphene covered surfaces practically undistinguishable.

The results presented in this paper highlight the high degree of complexity of the bonding and stability of the different intermediate surface species that are involved in the formation of a quasi free-standing graphene layer from ethylene adsorbed on the Ir(1 1 1) surface. The evolution of the different surface species is schematically presented in Fig. 4. In the following we compare our findings with those obtained on Pt(1 1 1) to discuss the surface reac-

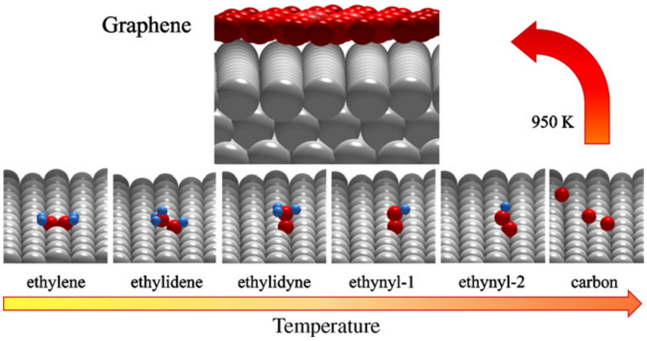

Fig. 4. Reaction scheme for the temperature evolution of an ethylene molecule on Ir(1 1 1).

tivity, the intermediates involved and the spectral contributions arising from non-equivalent carbon atoms and from vibrational features.

Our data confirm that Ir(1 1 1) is more reactive than Pt(1 1 1) in C–H bond breaking but only for certain processes. TP-XPS experiments on Pt(1 1 1) show unambiguously that the transition from ethylene to ethylidene is completed at 290 K, while on Ir(1 1 1) it is at 230 K. This corresponds to a lower (by ∼4 kcal/mol) activation energy for C_2H_4 to $CHCH_3$ conversion, compared to Pt(1 1 1) (15 kcal/mol) [24]. The main difference is that on Pt the conversion process is paralleled by the desorption of more than 50% of the saturated C_2H_4 layer, while on Ir the overall amount of carbon species remains almost constant up to about 370 K (see Fig. 2), in agreement with the small thermal desorption features observed on Ir(1 1 1) [12]. Therefore our results suggest that both ethylene and ethylidene are more strongly bound on Ir than on Pt.

On the contrary, the transformation of ethlydene to ethylidyne seems to occur at 320 K on both Pt(1 1 1) and Ir(1 1 1) surfaces. In this particular case we cannot exclude that the dissociation temperature is also affected by the different coverages of the coadsorbed species, which can modify the interactions among molecules and the availability of free surface sites for dissociation.

The high-temperature behaviour of the residual carbon atoms seems to be quite similar for Pt and Ir. Upon annealing at temperatures higher than ∼900 K a graphene layer is formed on both surfaces, whose interaction with the substrate is very small for Ir, even smaller for Pt if compared with other transition metal substrates like Rh, Ru and Ni [36].

Let us compare now the C 1*s* spectral features measured on Ir(1 1 1) and Pt(1 1 1) [16].

On both surfaces ethylene seems to adsorb most probably with the C axis parallel to the surface, because of the presence of one single component accompanied by its vibrational feature in the C 1*s* spectrum of ethylene. However our findings are not conclusive about the orientation of the C–C axis and we cannot exclude a small tilt of the molecule, which would results in undetectable difference in core level binding energies of non-equivalent C atoms. The main difference is in the ethylidene and ethylidyne spectra where the two carbon atoms exhibit in the Ir case different binding energies ($\Delta BE = 410$ meV for $CHCH_3$ and $\Delta BE = 400$ meV for C_2H_3), as expected being inequivalent (as sketched in Fig. 4). Two distinct C 1*s* components were also observed for ethylidyne on Rh(1 1 1) and Pd (1 1 1) surfaces, separated by 620 and 580 meV, respectively [19,20,37]. The difference between Pt and the other transition metal surfaces was explained as due to a different adsorption site for the CCH_3 species, leading to a different electron distribution within the molecule.

In conclusion we have shown that ethylene dissociation on Ir(1 1 1) proceeds through a complicated path that involves many intermediate surface species, revealed using the TP-XPS technique. The assignment of the different components was done on the basis of the core level binding energies, photoemission intensity thermal evolution, S factor, vibrational splitting and by close comparison with previous vibrational spectroscopy experiments.

Already at the dosing temperature of 170 K part of the ethylene molecules transform into a new species which is tentatively interpreted as ethylidene that represents the only species present on the surface between 235 and 250 K. At higher temperature the dehydrogenation process takes place and this species transforms completely into ethylidyne, which is stable on the surface from 310 to 370 K. A further increase of the temperature causes the complete dissociation of ethylidyne into C_2H species. The final dehydrogenation process that gives rise to adsorbed carbon, starts already at 500 K and is completed at 700 K. At 900 K the C 1*s* peak starts to shift and to narrow, a clear signature of graphene formation. The behaviour of the Ir $4f_{7/2}$ SCLS parallels that of the C 1*s* core level, thus confirming that the different species present on the surface interact differently with the underlying substrate.

Our results show that the high-resolution X-ray photoelectron spectroscopy technique is a powerful approach to study chemical reactions on solid surfaces. The recent achievement of our group, of an increased electron detection efficiency obtained with a new generation delay-line detector, can improve the data acquisition time up to the limit of few ms/spectrum. This, coupled with new, differentially pumped electron energy analysers for ambient pressure XPS, developed by other groups [38] opens the possibility for the in-situ study of short-living intermediate species in real pressure conditions, an important step towards the bridging of the so-called “materials and pressure gap”.

Acknowledgments

We acknowledge many stimulating discussions about graphene with D. Alfè. P. Lacovig is acknowledged for his support during the measurements. A.B. acknowledges financial support from Regione Friuli Venezia Giulia through the project “Catalizzatori nanostrutturati per la produzione di idrogeno e sperimentazione su prototipi di fuel-processor” and the precious technical support from Angst-Pfister.

References

[1] A.C.M. van den Broek, J. van Grondelle, R. van Santen, J. Catal. 185 (1999) 297.
[2] S.J. Cho, J. Lee, Y.S. Lee, D.P. Kim, Catal. Lett. 3–4 (2006) 181.
[3] E.W. Schmidt, Hydrazine and its Derivatives: Preparation, Properties, Applications, Wiley-Interscience, New York, 1984.
[4] M.A. Khan, O. Yang, Catal. Today 146 (2009) 177.
[5] D.F. Johnson, W.H. Weinberg, Science 261 (1996) 76.
[6] A.T. N'Diaye, S. Bleikamp, P.J. Feibelman, T. Michely, Phys. Rev. Lett. 97 (2006) 215501.
[7] E. Loginova, N.C. Bartelt, P.J. Feibelman, K.F. Mc Carty, New J. Phys. 10 (2008) 093026.
[8] J. Coraux, A.T. N'Diaye, N. Engler, C. Busse, D. Wall, N. Buckanie, F.-J. Meyer zu Heringdorf, R. van Gastel, B. Poelsema, T. Michely, New J. Phys. 11 (2009) 023006.
[9] A.H. Castro Neto, F. Guinea, N.M.R. Peres, N.M.R. Novoselov, A.K. Geim, Rev. Mod. Phys. 81 (2009) 109.
[10] P. Lacovig, M. Pozzo, D. Alfé, P. Vilmercati, A. Baraldi, S. Lizzit, Phys. Rev. Lett. 103 (2009) 166101.
[11] J.O. Sofo, R.D. Diehl, Physics 2 (2009) 84.
[12] B.E. Nieuwenhuys, D.I. Hagen, G. Rovida, G.A. Somorjai, Surf. Sci. 155 (1976) 59.
[13] Ts.S. Marinova, K.L. Kostov, Surf. Sci. 181 (1987) 573.
[14] Ts.S. Marinova, D.V. Chakarov, Surf. Sci. 192 (1987) 275.
[15] A. Baraldi, G. Comelli, S. Lizzit, M. Kiskinova, G. Paolucci, Surf. Sci. Rep. 49 (2003) 169.
[16] T. Fuhrmann, M. Kinne, B. Tränkenschuh, C. Papp, J.F. Zhu, R. Denecke, H.-P. Steinrück, New J. Phys. 7 (2005) 107.
[17] A. Baraldi, G. Comelli, S. Lizzit, D. Cocco, G. Paolucci, R. Rosei, Surf. Sci. L67 (1996) 367.
[18] S. Doniach, M. Šunjić, J. Phys. C 3 (1970) 185.
[19] J.N. Andersen, A. Beutler, S.L. Sorensen, R. Nyholm, B. Setlik, D. Heskett, Chem. Phys. Lett. 269 (1997) 371.
[20] A. Sandell, A. Beutler, A. Jaworowski, M. Wiklund, K. Heister, R. Nyholm, J.N. Andersen, Surf. Sci. 415 (1998) 411.
[21] C.J. Hirschmugl, G. Paolucci, F. Esch, S. Lizzit, K. Schindler, Surf. Sci. 488 (2001) 43.
[22] L.S. Cederbaum, W. Domcke, J. Chem. Phys. 64 (1976) 603.
[23] P. Cremer, C. Stanners, J.W. Niemantsverdriet, R. Shen, G. Somorjai, Surf. Sci. 328 (1995) 111.
[24] F. Zaera, T.V.W. Janssens, H. Öfner, Surf. Sci. 368 (1996) 371.
[25] A. Baraldi, J. Phys.: Condens. Matter 20 (2008) 93001.
[26] M. Bianchi, D. Cassese, A. Cavallin, R. Comin, F. Orlando, L. Postregna, E. Golfetto, S. Lizzit, A. Baraldi, New J. Phys. 11 (2009) 063002.
[27] B. Hammer, J.K. Nørskov, Surf. Sci. 343 (1995) 211.
[28] B. Hammer, J.K. Nørskov, Nature 376 (1996) 238.
[29] B. Hammer, O.H. Nielsen, J.K. Nørskov, Catal. Lett. 46 (1997) 31.
[30] B. Hammer, Topics Catal. 37 (2006) 3.
[31] U. Starke, A. Barbieri, N. Materer, M.A. Van Hove, G.A. Somorjai, Surf. Sci. 286 (1993) 1.
[32] K.J. Weestrate, A. Baraldi, L. Rumiz, S. Lizzit, G. Comelli, R. Rosei, Surf. Sci. 566–568 (2004) 486.

[33] E. Vesselli, A. Baraldi, F. Bondino, G. Comelli, M. Peressi, R. Rosei, Phys. Rev. B 70 (2004) 115404.
[34] E. Vesselli, M. Campaniello, A. Baraldi, L. Bianchettin, C. Africh, F. Esch, S. Lizzit, G. Comelli, J. Phys. Chem. C 112 (2008) 14475.
[35] S. Lizzit, Y. Zhang, K.L. Kostov, L. Petaccia, A. Baraldi, R. Larciprete, D. Menzel, K. Reuter, J. Phys. Condens. Matter 21 (2009) 134009.
[36] A.B. Preobrajenski, A.S. May Ling Ng, N. Vinogradov, Mårtensson, Phys. Rev. B 78 (2008) 073401.
[37] M. Wiklund, A. Beutler, R. Nyholm, J.N. Andersen, Surf. Sci. 461 (2000) 107.
[38] H. Bluhm, M. Hävecker, A. Knop-Gericke, E. Kleimenov, R. Schlögl, D. Teschner, V.I. Bukhtiyarov, D.F. Ogletree, M. Salmeron, J. Phys. Chem. B 108 (2004) 14340.